Influence of a ternary donor material on the morphology of a P3HT:PCBM blend for organic photovoltaic devices

ARTICLE *in* JOURNAL OF MATERIALS CHEMISTRY · JULY 2012

Impact Factor: 7.44 · DOI: 10.1039/C2JM31882B

5 AUTHORS, INCLUDING:

Florian Machui
Friedrich-Alexander-University of Erlangen-…
29 PUBLICATIONS **615** CITATIONS
SEE PROFILE

Ning Li
Friedrich-Alexander-University of Erlangen-…
34 PUBLICATIONS **848** CITATIONS
SEE PROFILE

Tayebeh Ameri
Friedrich-Alexander-University of Erlangen-…
72 PUBLICATIONS **2,134** CITATIONS
SEE PROFILE

Christoph J. Brabec
Friedrich-Alexander-University of Erlangen-…
398 PUBLICATIONS **26,345** CITATIONS
SEE PROFILE

Journal of Materials Chemistry

Cite this: J. Mater. Chem., 2012, 22, 15570

www.rsc.org/materials

PAPER

Influence of a ternary donor material on the morphology of a P3HT:PCBM blend for organic photovoltaic devices†

Florian Machui,*[a] Silke Rathgeber,[b] Ning Li,[a] Tayebeh Ameri[a] and Christoph J. Brabec[ac]

Received 26th March 2012, Accepted 13th June 2012
DOI: 10.1039/c2jm31882b

A comparison of grazing incidence wide-angle X-ray scattering (GiWAXS) and differential scanning calorimetric measurements (DSC) was used to identify the influence of a dominantly amorphous small band gap polymer material poly[2,6-(4,4-bis-(2-ethylhexyl)-4*H*-cyclopenta[2,1-*b*;3,4-*b*′]dithiophene)-*alt*-4,7(2,1,3-benzothiadiazole)] (PCPDTBT) on the crystallinity of a semi-crystalline polymer/fullerene composite. In binary blends the low band gap polymer does not influence the crystalline part of P3HT, but does influence the crystallinity of the fullerene. In ternary blends, a significant drop of the PCBM crystallinity is observed with increasing PCPDTBT content. Adding more than 20 wt% PCPDTBT to a P3HT:PCBM blend leads to a dramatic reduction of device efficiency, mainly due to short circuit current density and fill factor losses. This deterioration is attributed to the fact that addition of more than 20 wt% PCPDTBT to the host system strongly reduces crystallinity of the fullerene phase and electron transport in the ternary system.

1. Introduction

The increasing interest in inexpensive renewable energy sources continues to encourage new approaches for efficient, low-cost photovoltaic devices. Solution-processed organic photovoltaic (OPV) devices offer different advantages for fabrication of large areas.[1] Significant advancements have led to certified efficiencies of 8.3%.[2,3] The most common analyzed concept for the active layer is the bulk heterojunction (BHJ), which consists of an interpenetrating network of a hole conductor and an electron acceptor exhibiting an increased interface compared to that of a bilayer approach.[4] A spontaneous phase separation during film formation forms a specific nanostructure which is decisive for the charge transport and the charge separation. Therefore the key for high OPV performance is to control the morphology of the polymer–fullerene blends.[5] Poly-(3-hexylthiophene-2,5-diyl) (P3HT), a conjugated semi-crystalline organic semiconductor, and [6,6]-phenyl-C_{61}-butyric acid methyl ester (PCBM), a fullerene derivative, are the two most frequently reported materials used in OPV devices. Their phase behavior and structure–property relation were discussed in great detail.[6–15] We have recently suggested the use of ternary blends to expand the absorption spectra towards the near infrared region to increase the short circuit current density of a cell.[16] Various material and device specifications need to be fulfilled for ternary sensitization. The absorption of the near infrared sensitizer should be complementary to the absorption spectra of P3HT and the position of the electronic levels with respect to those of P3HT and PCBM must facilitate photoinduced charge transfer between all components. Poly[2,6-(4,4-bis-(2-ethylhexyl)-4*H*-cyclopenta[2,1-*b*;3,4-*b*′]dithiophene)-*alt*-4,7(2,1,3-benzothiadiazole)] (PCPDTBT) was suggested as a highly promising near IR sensitization candidate due to its ideal energy level and charge carrier properties.[16–18] However, despite successfully demonstrating IR sensitization, PCPDTBT showed nearly no significant efficiencies increase. We have recently discussed that the morphology formation of such a ternary system is far more complex than that of binary ones.[19]

One method to determine the thermal behavior of the microstructure and the crystallinity is differential scanning calorimetry (DSC). This is a fundamental thermo analytical technique in material and polymer science. For semi-crystalline semiconductor blends, such as mixtures of P3HT and PCBM, reconstruction of the phase diagram by DSC is done by analyzing the heat flow of the melting or crystallization peaks.[14,20,21] The crystallinity of a material can be determined from DSC measurements using eqn (1) and (2) with ΔH as enthalpy change, C_p as heat capacity with constant pressure, K as crystallinity, ΔH_m as measured melting enthalpy change and ΔH_m^0 as enthalpy change for a 100% crystalline material.

$$\Delta H = \int C_p \times dT \quad (1)$$

[a]*I-MEET (Institute of Materials for Electronics and Energy Technology) University Erlangen-Nuremberg, Martensstrasse 7, 91058 Erlangen, Germany. E-mail: Florian.Machui@ww.uni-erlangen.de*
[b]*Institute for Natural Sciences, Physics Department, University of Koblenz-Landau, Universitätsstraße 1, 56070 Koblenz, Germany*
[c]*Bavarian Center for Applied Energy Research (ZAE Bayern), Am Weichselgarten 7, 91058 Erlangen, Germany*
† Electronic supplementary information (ESI) available. See DOI: 10.1039/c2jm31882b

$$K = \frac{\Delta H_m}{\Delta H_m^0} \times 100\ [\%] \quad (2)$$

Malik and Nandi analyzed the melting enthalpy of different poly-alkylthiophenes. The melting enthalpy of a perfect P3HT crystal was identified as 99.0 J g^{-1}.[22] Binary blends of P3HT:PCBM were analyzed by Müller *et al.* and Kim *et al.*[13,14] The addition of a third component, especially of a weakly crystalline material, makes the thermal behavior of such ternary blends around the melting point significantly more complex. Miscibility estimates were obtained from measurements of the melting point depression, which were analyzed with DSC experiments.[23] Miscibility between P3HT and PCBM suppresses fullerene crystallization. The nanoscale morphology in these materials is controlled by crystallization of the polymer within the partially miscible blend during drying. The crystallization of P3HT leads to the characteristic length scales of the mesostructure and to macroscopic phase separation by enriching the amorphous polymer phase with fullerene. Furthermore, depth profiles of P3HT:PCBM bilayers showed interdiffusion of both materials even after short annealing times. Therefore it was concluded that pure amorphous phases do not exist in BHJ or annealed bilayer devices. Energy-filtered transmission electron microscopy (EFTEM) and grazing incidence small angle X-ray scattering (GiSAXS) measurements were used for morphological investigations, showing local P3HT concentrations in PCBM-rich domains. This was interpreted as partially miscibility. Moreover, it is found that, while no intercalation occurs in the crystalline phase of P3HT, amorphous portions of P3HT contain significant concentrations of PCBM.[13,24]

Mayer *et al.* analyzed the intercalation of fullerenes between polymer side chains of different amorphous and semi-crystalline polymers.[25] X-ray diffraction measurements were used to demonstrate the formation of stable, well-ordered bimolecular crystals of fullerene intercalated between the side-chains of the semiconducting polymers. It was shown that fullerene intercalation occurred in blends with both amorphous and semi-crystalline polymers when there is enough free volume between the side-chains to accommodate the fullerene molecule. PCBM intercalating between the side chains of P3HT was not possible. When intercalation occurs, a high level of fullerene-loading is necessary to create the phase separation needed for efficient BHJ solar cells, which leads to optimum blend ratios near 1 : 3–1 : 4 wt% polymer : fullerene in contrast to an optimum near 1 : 1 wt% in systems where intercalation cannot occur.

Khlyabich *et al.* analyzed the influence of a third acceptor component on device performance.[26] For a donor–acceptor ratio of 1 : 1 wt% with varying the ratio of PCBM to indene-C_{60} bisadduct ($IC_{60}BA$), the open circuit voltage (V_{OC}) increased linearly with increasing $IC_{60}BA$ content. This suggested that in ternary blends the V_{OC} is not limited to the smallest V_{OC} but can be varied between the extreme V_{OC} values without influencing short circuit current density (j_{SC}) or fill factor (FF).

Ternary systems containing P3HT, PCPDTBT, and PCBM were investigated by Li *et al.* using DSC.[19] The phase diagram of the binary system P3HT:PCBM showed a simple eutectic point. Furthermore, it was found that even small amounts of the dominantly amorphous polymer PCPDTBT decrease the crystallinity but do not affect the position of the eutectic point in ternary blends. A comparison with cell performance showed an excellent correlation between the phase behavior of the binary and ternary blends with the photovoltaic performance.

In this manuscript we report a detailed investigation of the microstructure formation of ternary blends. Most relevant is the observation of a dramatic decrease of fullerene crystallinity upon addition of PCPDTBT. This was analyzed by means of differential scanning calorimetric and grazing incidence wide angle scattering methods. This crystallinity decrease results in reduced short circuit current densities and lower fill factors of the devices when more than 20 wt% PCPDTBT content is added to the P3HT:PCBM binary system.

2. Experimental

P3HT (with weight average molar mass (M_w) = 65.6 kg mol^{-1}, polydispersity (PD) = 2.04, and regioregularity (RR) = 96.6 from Merck), and PCBM (with purity of >99% from Solenne BV) were used as received. PCPDTBT (M_w = 47.0 kg mol^{-1}, PD = 1.34) was supplied by Konarka.

DSC samples were measured with a Q1000 from TA Instruments. Powders (P3HT, PCBM and PCPDTBT) were dissolved in chlorobenzene with a concentration of 1 wt% and stirred at 60 °C for at least 1 hour. The solutions were mixed with different ratios and stirred for at least another hour. The homogeneous solutions were drop cast on clean substrates and dried under air. Free standing films were taken of the substrates and samples of approximately 5 mg were weighed with a microbalance and filled into DSC pans. For DSC measurements, temperature ranges from −50 °C to 330 °C and heating and cooling rates of 10 K min^{-1} were used. The enthalpy determination was calculated using software TA Universal Analysis.

We performed grazing incidence wide-angle X-ray scattering experiments at the BW4 beam line, at HASYLAB at DESY in Hamburg, Germany. Experiments were carried out in a pseudo-grazing incidence configuration at a wavelength of $\lambda = 0.138$ nm with a band width of 10^{-4} and a spot size of 78 μm × 46 μm in horizontal and vertical directions, respectively. The incident polar angle has been set to $\alpha_i = 0.20°$. Two-dimensional detector patterns were collected with exposure times of 900 s. For the measurements on the neat films (Fig. 2) and those prepared from the ternary blends (Fig. 4) a hybrid pixel array detector (Pilatus 300k, DECTRIS, pixel size 172 μm) was used. Measurements on the films prepared from polymer:PCBM binary blends (Fig. 3) were performed using a CCD-detector (MAR165CCD, pixel size 79.1 μm). The detector to sample distance was determined by means of a silver behenate standard. Data are corrected for background scattering from the silicon substrate and are normalized to the film thicknesses and incoming flux in order to allow for a comparison of peak intensities between different samples. Data are shown in (q,Φ)-presentations. Here, $q = 2\pi/d$ is the overall momentum transfer which can be directly related to the distance d of the corresponding scattering planes. Φ denotes the angle between the directions parallel ($\Phi = 0°$) and perpendicular ($\Phi = 90°$) to the sample surface. For more details on the experimental setup and data conversion see ref. 27.

The organic BHJ photovoltaic devices were fabricated on indium tin oxide (ITO) coated glass substrates. The following layer sequence was used: poly(3,4-ethylenedioxythiphene) doped

with polystyrene sulfonate (PEDOT:PSS)/active layer/Ca/Ag. PEDOT:PSS was doctorbladed with approximately 60 nm thickness and subsequent blading of the semiconductor layer with approximately 100 nm thickness. For the active layer, devices were prepared from solutions containing a donor–acceptor ratio of 1 : 1 wt% with 2 wt% total concentrations in chlorobenzene. Layers of 15 nm Ca and 100 nm Ag were deposited as the top electrode. For a better performance, the solar cells containing P3HT were annealed at 140 °C for 5 min. The active area of the investigated devices was 0.1 cm^2. Current density–voltage (*jV*) characteristics were measured with a source measurement unit from BoTest. Illumination was provided by an Oriel Sol 1A solar simulator with AM1.5 spectra at 0.1 W cm^{-2}.

Mobility measurements were performed using a space charge limited current (SCLC) method. For the electron only devices, active layer materials were measured within aluminium doped zinc oxide and Ca/Ag electrode layers. For the hole only devices active layer materials were measured within two PEDOT electrode layers.

3. Results and discussion

3.1 Differential scanning calorimetry

3.1.1 Binary blends. The DSC thermograms received from the first run can be seen in Fig. S4 in the ESI†. The heating curves of P3HT and PCBM show distinct melting peaks, confirming the relatively high crystallinity of both neat materials.[13] The melting temperatures of both materials, identified by the peak temperatures, were determined as 241 °C and 282 °C respectively. The DSC heating curve of neat PCPDTBT only shows a small melting peak with a peak temperature of 293 °C. In the DSC curves of the binary mixtures of P3HT and PCPDTBT the melting peak of P3HT is always observed. No temperature dependent shift of the peak is recognizable. Since the PCPDTBT melting peak is quite small, it is hardly detected in the blends. With decreasing P3HT content peak size decreases, relating to the smaller amount in the blend. The normalized enthalpy of this system, as determined by integrating the area beneath the melting peak, shows a linear relationship with nearly a slope of 1 (Fig. 1). This shows that PCPDTBT does not influence the P3HT crystallinity in the binary system and could be a sign that in the ternary system PCPDTBT affects mainly the PCBM crystalline domains rather than P3HT ones. PCPDTBT obviously does not intercalate into the crystalline P3HT domains, but rather mixes with the amorphous phase. The mixing behavior of PCBM and PCPDTBT is totally different.

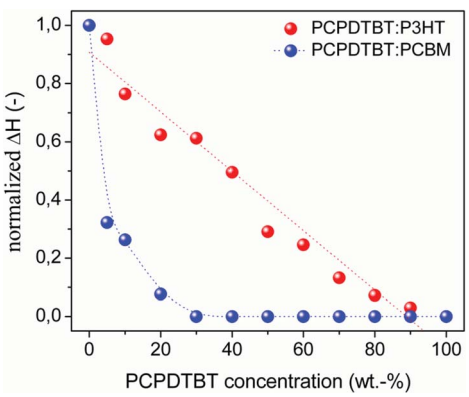

Fig. 1 Normalized enthalpy change determined by integral P3HT and PCBM of melting peak area in binary blends of PCPDTBT:P3HT and PCPDTBT:PCBM, respectively.

In contrast, binary blends of PCBM with PCPDTBT show no PCBM melting peak for blends with >30 wt% PCPDTBT content. The peak height of PCBM enthalpy dramatically drops with increasing PCPDTBT content, and small temperature shifts of the melting temperature are recognizable. Again, the whole PCBM crystal melting enthalpy was determined. Fig. 1 shows a strong, super linear decrease of the normalized enthalpy already at a 5 wt% PCPDTBT content. This decreasing PCBM crystallinity indicates that PCBM, indeed, does intercalate in PCPDTBT. According to Mayer *et al.* the percent of intercalated fullerene y can be calculated according eqn (3) with x as the weight fraction of fullerene added to the blend for the formation of equal volumes, ζ as the molecular weight (M_w) ratio of the monomer of the polymer to the fullerene unit and n as the number of fullerenes per monomer in the intercalated phase.[25]

$$y = (1 - x) \times \zeta \times n \quad (3)$$

By using M_w of the monomer unit of PCPDTBT of 548.56 g mol^{-1} and M_w of PCBM of 910.9 g mol^{-1}, $n \approx 2$ for PCPDTBT and PCBM and $x = 73$ wt% (according to ref. 25), 32.5 wt% of the fullerene can be intercalated. In our measurements we used 50 wt% fullerene content, which results in a calculated maximum intercalated fullerene content y of 60.2 wt% and is dependent on the PCPDTBT concentration in the system, since PCBM is not able to intercalate in P3HT. The theoretical maximum intercalated fullerene content can be calculated with eqn (4) with $c_{PCPDTBT}$ as the concentration of PCPDTBT in the system.

$$y = n \times c_{PCPDTBT} \times \zeta \quad (4)$$

This results in a maximum intercalating fullerene content dependent on the PCPDTBT concentration multiplied by a factor of 1.20.

We have already discussed binary blends of P3HT and PCBM in ref. 19. Here it was reported that both neat materials show distinct melting peaks. A P3HT melting peak is recognizable up to 20 wt% P3HT, and this peak is slightly shifted towards lower temperatures. For PCBM a melting peak is recognizable up to 50 wt% PCBM. In comparison to PCPDTBT:PCBM the drop in crystallinity is much lower.

3.1.2 Ternary blends. For solar cell applications a donor–acceptor ratio of 1 : 1 is frequently reported for non-intercalating composites.[28] In the case of ternary blends, this ratio is typically kept constant and the ratio of the donors P3HT and PCPDTBT is varied.[16] Fig. S1c in the ESI† shows the thermograms of ternary mixtures with a fixed ratio of 50 wt% PCBM and varied ratios of P3HT and PCPDTBT. Furthermore, the heat flow of neat P3HT and PCBM is shown as a comparison.

The enthalpy change determined by the peak area of the melting peaks shows comparable values for neat P3HT and PCBM (17.9 J g^{-1} and 17.1 J g^{-1} respectively). Binary blends of P3HT:PCBM with a ratio of 50 : 50 by weight fraction show a

decrease of both enthalpies, especially for the PCBM enthalpy (lower than 2 J g^{-1}). Therefore crystallinity is dramatically reduced. By the addition of PCPDTBT with a polymer to fullerene ratio of 50 : 50 by weight fraction the P3HT enthalpy is further decreased. In any case, this is more than expected compared to the weight fraction. Therefore the addition of PCPDTBT slightly decreases the crystallinity of P3HT, which was not recognized in the binary blends of P3HT and PCPDTBT. PCBM enthalpy was hardly recognizable in the ternary blends. For both cases, addition of P3HT and PCPDTBT, the crystallinity of PCBM is diminished. Summarizing, DSC results show that in binary blends PCPDTBT does not influence the crystalline part of P3HT, but does influence the crystallinity of the fullerene. In ternary blends with a donor–acceptor ratio of 1 : 1 wt% definite predications are difficult to make.

3.2 Grazing incidence wide-angle X-ray scattering

Fig. 2 shows the two-dimensional detector pattern obtained for the neat polymer and PCBM films. The degree of order in the as coated P3HT films is high. The interlayer peak ($q = 3.96$ nm^{-1}, $d = 1.59$ nm, $\phi = 90°$) originating from the layered structure, built by the conjugated backbones separated by layers comprising the alkyl side chains, is narrow and high in intensity. Higher order peaks are also visible. The peak ($q = 16.8$ nm^{-1}, $d = 0.374$ nm, $\phi = 0°$) originating from $\pi\pi$-stacking perpendicular to the interlayer stacking is also observed. Annealing of the P3HT films does not result in a significant improvement in the degree of order (compare ESI, Fig. S1†).

Compared to P3HT the PCPDTBT is less organized. Note that the detector pattern is plotted on a reduced intensity scale. The peak at $q = 5.84$ nm^{-1} ($d = 1.08$ nm, $\phi = 90°$) is attributed to domains with a preferred edge-on orientation relative to the substrate.[29] However, there is also a large fraction of domains with a preferred face-on orientation ($q = 16.4$ nm^{-1}, $d = 0.383$ nm, $\phi = 90°$). The peak at $q = 10.6$ nm^{-1} ($d = 0.59$ nm, $\phi = 90°$) indicates weak correlations between different chains along the conjugated backbones. The length scale of the *d*-spacing corresponds well with the approximate distance between the sulfur atoms in the backbone.

In accordance with previously reported results on spin coated PCBM films the doctorbladed PCBM film shows three broad peaks ($q = 7.3$ nm^{-1}, 13.8 nm^{-1} and 20.6 nm^{-1}).[27] The peaks originate from a superposition of several broad peaks originating from different lattice planes (compare to wide-angle X-ray scattering results from crystalline PCBM).[30] Since higher order scattering features are observed, the PCBM is not amorphous but order is not long ranged. The scattering is isotropic and hence there is no preferred orientation of the PCBM domains relative to the substrate. For the following discussion we will take the peak intensity of the main PCBM peak at about 14 nm^{-1} as a measure for the degree of phase separation (at the same PCBM content) or more generally as a measure for the amount of neat PCBM phase. In order to allow for a comparison of the spectra obtained for the ternary and binary mixtures to that of the neat PCBM film, the intensities of the blend films are scaled according to the volume fraction of PCBM which is on average 43 ± 2 vol% (see ESI†).

Fig. 3 shows the two-dimensional detector pattern obtained for the films prepared from the binary polymer:PCBM mixtures. In the P3HT:PCBM 50 : 50 wt% film the degree of order of the polymer phase is preserved compared to that of the neat P3HT film. It seems that the crystallinity close to the film surfaces is somewhat enhanced (interlayer stacking peak is higher). However, the isotropic contribution is reduced, indicating that the ordering tendency in the bulk of the thin film is lower. For the PCPDTBT the ordering of the polymer phase is significantly reduced. A weak isotropic contribution at $q = 5.84$ nm^{-1} and some residual scattering from face-on domains at $q = 16.4$ nm^{-1} is observed. These results are in accordance with those obtained from DSC measurements on the binary mixtures. For both systems the PCBM is most likely incorporated into the polymers phase, also leading to a reduction of the crystallinity of the P3HT in the bulk of the P3HT:PCBM film. However, the less organized PCPDTBT obviously shows a higher intercalation tendency than that of the more crystalline P3HT. The peak height of the main PCBM peak of the P3HT:PCBM film is comparable to that of the neat PCBM film, whereas the intensity of that of the PCPDTBT:PCBM film is clearly reduced. Here, a difference to the DSC results could be found. The reduced PCBM crystallinity in binary mixtures with P3HT was also found in DSC measurements in ref. 13 and 14. One reason for the differences could be that the main PCBM peak corresponds to nearest neighbor correlations. Thus GiWAXS rather measures the amount of neat PCBM phase but not necessarily its crystallinity.

In the films prepared from the ternary mixtures (see Fig. 4) the crystallinity of the P3HT is further drastically reduced. Obviously the presence of the PCPDTBT is detrimental for the ordering process of the P3HT. This is in accordance with the DSC results

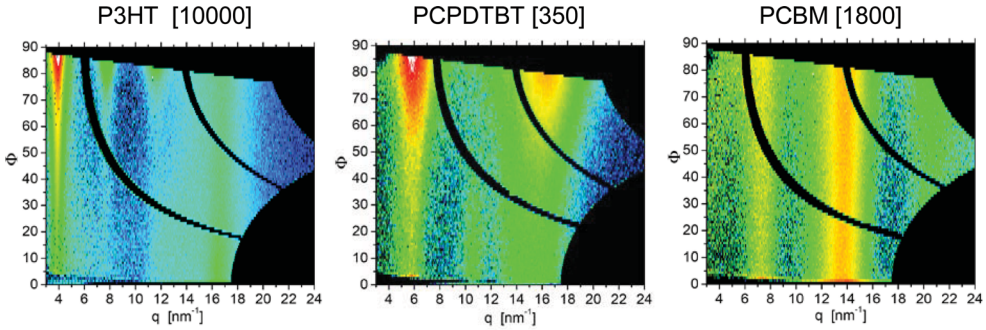

Fig. 2 Two-dimensional GiWAXS detector pattern: films prepared from the neat polymers and PCBM:P3HT (left), PCPDTBT (middle) and PCBM (right). Intensity scales are given in brackets.

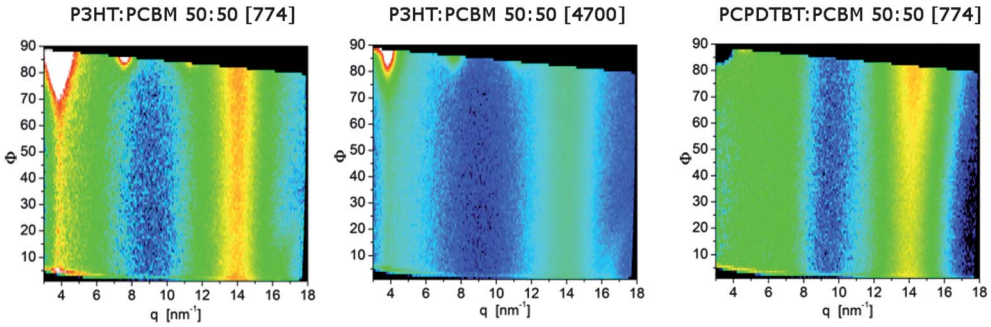

Fig. 3 Two-dimensional GiWAXS detector patterns: films prepared from P3HT:PCBM (left, middle) and PCPDTBT:PCBM (right) 50 : 50 wt% binary blends. Intensity scales (given in brackets) are adjusted according to the volume fraction of 43 vol% of PCBM [774] and 47 vol% of P3HT [4700] in order to allow a direct comparison to the spectra obtained for the corresponding neat films. Intensity scales are given in brackets.

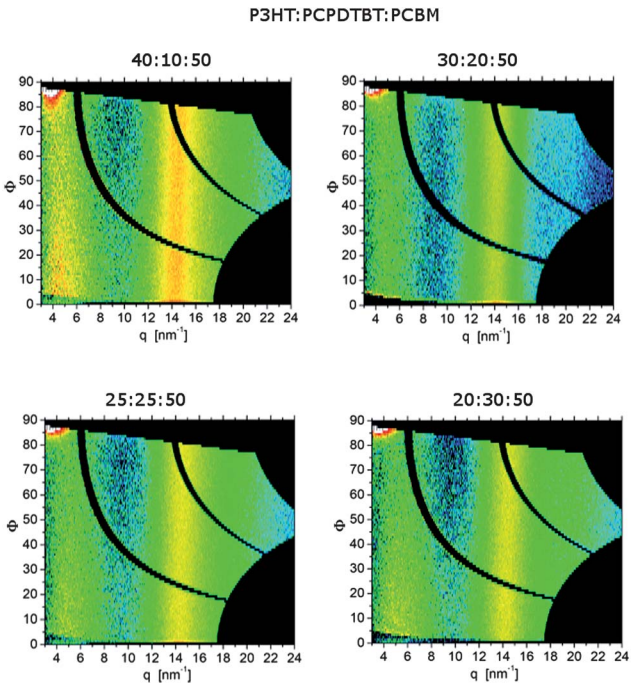

Fig. 4 Two-dimensional GiWAXS detector patterns: films prepared from P3HT:PCPDTBT:PCBM $x : 50 - x : 50$ wt% ternary blends $x = 40$, 30, 25, 20 wt%. Intensity scales are adjusted according to a volume fraction of PCBM (43 wt%) to 774 in order to allow a direct comparison to the spectrum obtained for the neat PCBM film.

on binary P3HT:PCPDTBT mixtures. As for the binary mixtures, no significant scattering signal from the PCPDTBT is detectable. For the system P3HT:PCPDTBT:PCBM 40 : 10 : 50 wt% the degree of phase separation is high. The PCBM signal is comparable to that of the neat PCBM films. Increasing the PCPDTBT fraction to 20 wt% leads to a reduction of the amount of PCBM phase. The PCBM is most likely incorporated into the polymer phase. The scattering results do not allow for unambiguous conclusions as to whether incorporation takes place preferably in one of the polymer components but the decrease in the degree of phase separation is accompanied by a significant further decrease in the P3HT peak intensity (more than expected from the decrease in P3HT fraction). The results obtained for the blend with a PCPDTBT fraction of 25 wt% are comparable to those obtained for the film with 20 wt%. Increasing the amount of PCPDTBT further to 30 wt% seems to enhance phase separation which is, however, still lower than that observed for the film with 10 wt% but approaches the conditions observed for the film prepared from the binary PCPDTBT:PCBM mixture.

Scheme 1 summarizes our comprehension of the morphological evolution for PCPDTBT addition into the P3HT:PCBM binary blend. The binary blend system contains crystalline P3HT and PCBM parts embedded in an amorphous matrix of both components.[14] Addition of 0–20 wt% PCPDTBT decreases the crystallinity of PCBM as observed by DSC and GiWAXS measurements. Since the impact on P3HT crystallinity is relatively small it is concluded that PCPDTBT is dominantly embedded in the amorphous part of P3HT. With higher amounts of PCPDTBT the crystallinity of PCBM is strongly damaged and hardly recognizable with DSC and GiWAXS measurements. Furthermore, the P3HT crystallinity is diminished as compared to that of the binary blend. At this high PCPDTBT concentration the amorphous part from all three materials becomes the main phase with small inclusions of P3HT and PCBM crystals.

3.3 SCLC measurements

Following our analysis from DSC and GiWAXS one would expect that the reduced PCBM crystallinity in ternary blends may lead to reduced transport properties. SCLC measurements are a commonly used tool to determine the mobility of organic materials. Different conditions have to be fulfilled to reach SCLC requirements, like type of carriers, low mobility, constant mobility and dielectric permittivity through all the sample and strongly preferentially and trap-free charge transport.[31–33] Using the Mott–Gurney law under the assumption that deep localized states are negligible and that mobility is field independent, the SCL current density (J_{SCL}) is given by eqn (5), with ε_0 as the electric permittivity of free space, ε_r the relative dielectric constant of the active layer, μ the charge carrier mobility, L the thickness of the device and V_{in} is the voltage dropped across the sample given by eqn (6).[34]

$$J_{SCL} = \frac{9}{8}\varepsilon_0\varepsilon_r\mu\frac{{V_{in}}^2}{L^3} \quad (5)$$

$$V_{in} = V - V_{bi} - V_{rs} \quad (6)$$

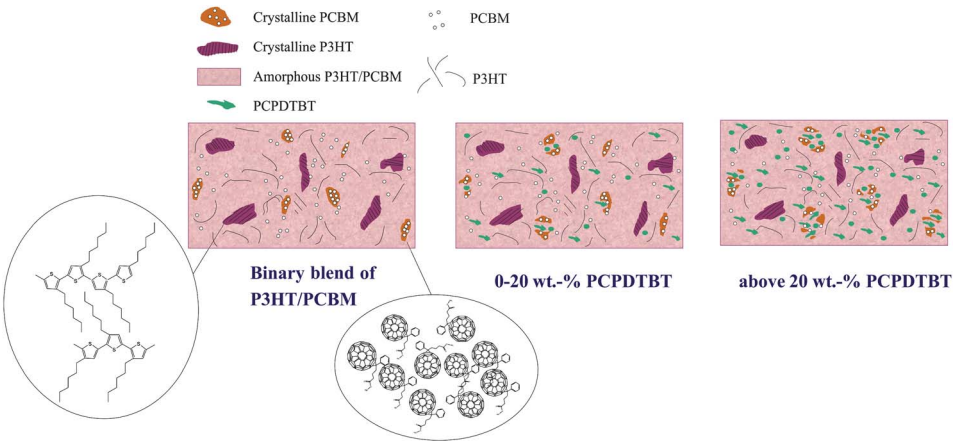

Scheme 1 Influence of PCPDTBT addition on morphology of the P3HT:PCBM binary blend.

where V is the applied voltage, V_{bi} the built-in voltage and V_{rs} is the voltage drop due to the series resistance of the contacts. In the case of a field dependent mobility as described by the Poole–Frenkel effect, the SCL current density is given by the modified Mott–Gurney equation:

$$J_{SCL} = \frac{9}{8}\varepsilon_0\varepsilon_r\mu\frac{{V_{in}}^2}{L^3}\exp\left(\frac{0.89\beta}{\sqrt{L}}\sqrt{V}\right) \quad (7)$$

where β is the electric field-activation factor of mobility and accounts for the degree of disorder, particularly the energetic level distribution of the carrier hopping sites in the material, *i.e.*, a smaller β indicates a lower degree of energetic disorder.[35] The field dependent SCLC expression yielded a reasonably good fit to the measured jV curves of single-carrier devices. As can be seen in Table 1, with increasing PCPDTBT content the mobility decreases in the electron only devices. This is even more dramatic for a PCPDTBT content of 40 wt% in the ternary system. For the hole only devices this effect cannot be observed. Here the mobility is still of the same magnitude. These findings correlate with a significant influence of PCPDTBT on the fullerene crystallinity, which results in a decreased electron mobility, whereas the P3HT crystallinity and therefore the hole mobility is not affected.

3.4 Comparison with device efficiencies

Small amounts of PCPDTBT in P3HT:PCBM blends have been reported to improve the power conversion efficiency (PCE) by Koppe *et al.*[16] In our previous studies the sensitization of P3HT by small amounts of PCPDTBT was confirmed but the increase in solar cell performance was negligible. Müller *et al.* reported that the maximum current densities are found at slightly hypo-eutectic concentrations ($c < c$ eutectic) in terms of polymer content.[14] The main reason for the hypo-eutectic fullerene concentration is the formation of percolated paths, which need an over excess of PCBM.[36,37] The best ratios for PCPDTBT:PCBM binary solar cells were reported for ratios of 1 : 3 and 1 : 4, depending on the processing conditions.[18,38,39] To correlate the electrical properties of ternary blends with their phase behavior, photovoltaic devices with a constant polymer- : fullerene ratio of 50 : 50 wt% under identical processing conditions (solvent, concentration, annealing) are studied. Fig. 5 shows the jV curves of the photovoltaic devices under AM1.5, 100 mW cm^{-2} illumination. 0 wt% PCPDTBT denotes neat P3HT:PCBM solar cells. Annealing in principle improves the device performance. A remarkable drop in V_{OC} has been observed which is surpassed by the gains in j_{SC}. There is a striking difference for solar cells with higher PCPDTBT content (over 20 wt%). These cells have significantly lower j_{SC} and fill factors. Obviously, addition of more than 20 wt% PCPDTBT results in a dramatic change in the P3HT:PCBM morphology. Fig. 6 directly plots the normalized device parameters (V_{OC}, j_{SC}, FF and PCE) as a function of the PCPDTBT ratio. J_{SC} slightly increases with

Table 1 Mobility measurement results

Composition of the active layer P3HT: PCPDTBT:PCBM/wt%	Electron only devices/cm^2 V^{-1} s^{-1}	Hole only devices/cm^2 V^{-1} s^{-1}
50 : 0 : 50	2.3×10^{-3}	2.4×10^{-4}
40 : 10 : 50	2.7×10^{-4}	2.8×10^{-4}
10 : 40 : 50	5.0×10^{-5}	1.5×10^{-4}

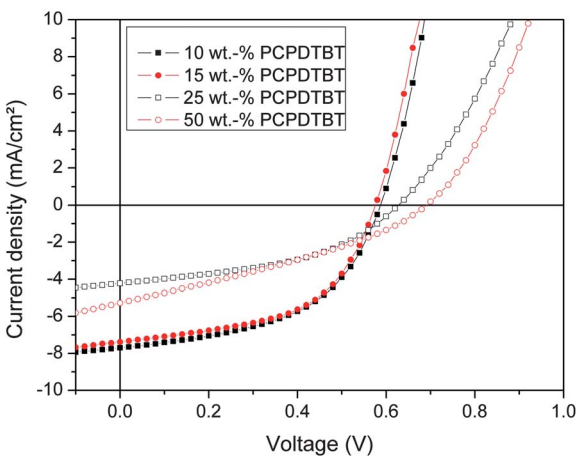

Fig. 5 Illuminated jV curves of P3HT:PCPDTBT:PCBM ternary solar cells with a polymer : fullerene ratio of 50 : 50 wt%.

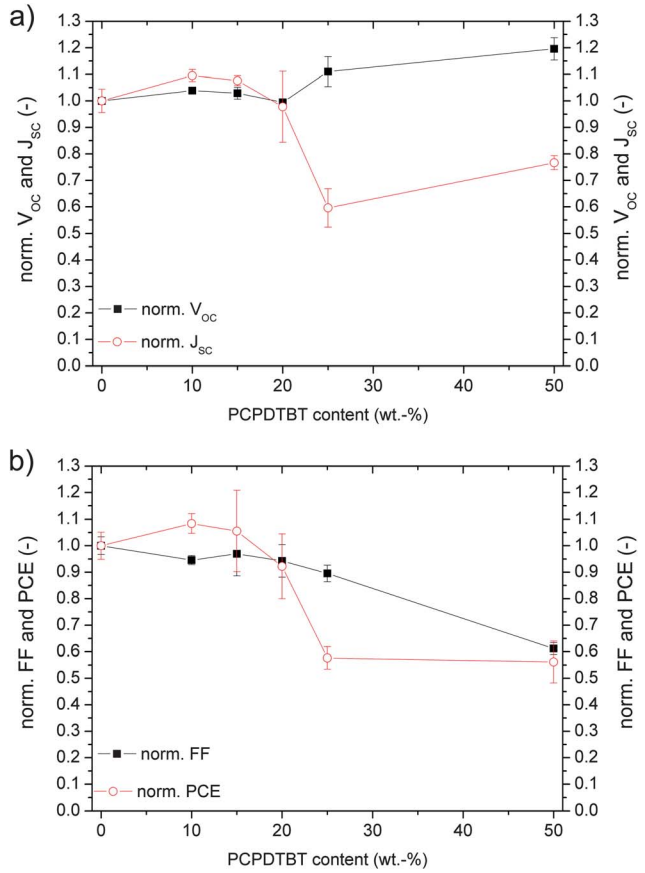

Fig. 6 (a) Normalized V_{OC} and j_{sc} and (b) normalized FF and PCE of photovoltaic devices *versus* the PCPDTBT ratio for ternary blends with a constant polymer : fullerene ratio of 50 : 50 wt%. The solar cells were tested under AM1.5 spectra at 0.1 W cm^{-2} illumination. As a reference, 0 wt% PCPDTBT in the blend system was chosen.

higher PCPDTBT content due to the enhanced absorption in the NIR region which was already reported by Koppe *et al.*[16] More than 20 wt% PCPDTBT content leads to a j_{SC} drop, resulting from the above discussed morphology changes in the ternary system. V_{OC} increases with higher PCPDTBT content and the fill factor drops for PCPDTBT contents higher than 20 wt%. For the resulting PCE up to 20 wt% PCPDTBT does not dramatically change the efficiency. With higher PCPDTBT content, PCE significantly decreases, mainly due to the lower j_{SC}. This is in excellent agreement with the findings from the phase diagrams in ref. 19, where addition of more than 20 wt% PCPDTBT resulted in completely amorphous blends. Furthermore, our GiWAXS measurements and DSC results confirm these results. In summary, we find good correlation between the morphological changes of the semiconductor blends and their photovoltaic properties.

4. Conclusion

Grazing incidence wide-angle X-ray scattering (GiWAXS) and differential scanning calorimetry (DSC), space charge limited current (SCLC) transport analysis and solar cell trials were used to analyze the mechanisms of the NIR sensitization in ternary blends. In detail, the influence of a dominantly amorphous small band gap polymer poly[2,6-(4,4-bis-(2-ethylhexyl)-4*H*-cyclopenta[2,1-*b*;3,4-*b*′]dithiophene)-*alt*-4,7(2,1,3-benzothiadiazole)] (PCPDTBT) on the crystallinity of a semi-crystalline polymer poly-(3-hexylthiophene) (P3HT) and a fullerene derivative [6,6]-phenyl-C_{61}-butyric acid methyl ester (PCBM) was investigated. According to DSC measurements, addition of the low band gap polymer does not influence the crystalline part of P3HT. On the contrary, the crystallinity of the fullerene is strongly reduced by PCPDTBT addition. In ternary blends with a donor–acceptor ratio of 1 : 1, a significant drop of PCBM crystallinity is again formed with increasing PCPDTBT content. It was concluded that additional PCPDTBT mainly interacts and intermixes with the crystalline phases of the fullerene. Indeed, devices showed a slight performance increase with PCPDTBT contents below 20 wt%. Higher amounts led to a drop of j_{SC} and FF, resulting in overall lower PCEs. This mechanism is in excellent agreement with the DSC, GiWAXS and SCLC analysis.

Acknowledgements

The authors gratefully acknowledge the support of the Cluster of Excellence 'Engineering of Advanced Materials' at the University of Erlangen-Nuremberg, which is funded by the German Research Foundation (DFG) within the framework of its 'Excellence Initiative' and the project near IR sensitization of polymer fullerene solar cells in the framework of SPP1355 of the DFG.

Notes and references

1 C. J. Brabec, *Sol. Energy Mater. Sol. Cells*, 2004, **83**, 273.
2 Heliatek, http://www.heliatek.com.
3 Konarka, http://www.konarka.com.
4 H. Hoppe, M. Niggemann, C. Winder, J. Kraut, R. Hiesgen, A. Hinsch, D. Meissner and N. S. Sariciftci, *Adv. Funct. Mater.*, 2004, **14**, 1005–1011.
5 T. Stübinger and W. Brütting, *J. Appl. Phys.*, 2001, **90**, 3632.
6 H. Hoppe and N. S. Sariciftci, *J. Mater. Res.*, 2004, **19**, 1924.
7 M. D. McGehee and M. A. Topinka, *Nat. Mater.*, 2006, **5**, 675.
8 J. Y. Seong, K. S. Chung, S. K. Kwak, Y. H. Kim, D. G. Moon, J. I. Han and W. K. Kim, *J. Korean Phys. Soc.*, 2004, **45**, 5914.
9 H. Frohne, S. E. Shaheen, C. J. Brabec, D. C. Muller, N. S. Sariciftci and K. Meerholz, *ChemPhysChem*, 2002, **3**, 795.
10 D. Chirvase, J. Parisi, J. C. Hummelen and V. Dyakonov, *Nanotechnology*, 2004, **15**, 1317.
11 H. Hoppe, M. Niggemann, C. Winder, J. Kraut, R. Hiesgen, A. Hinsch, D. Meissner and N. S. Sariciftci, *Adv. Funct. Mater.*, 2004, **14**, 1005.
12 S. H. Park, A. Roy, S. Beaupré, S. Cho, N. Coates, J. S. Moon, D. Moses, M. Leclerc, K.-H. Lee and A. J. Heeger, *Nat. Photonics*, 2009, **3**, 297.
13 J. Y. Kim and C. D. Frisbie, *J. Phys. Chem. C*, 2008, **112**, 17726–17736.
14 C. Müller, T. A. M. Ferenczi, M. Campoy-Quiles, J. M. Frost, D. D. C. Bradley, P. Smith, N. Stingelin-Stutzmann and J. Nelson, *Adv. Mater.*, 2008, **20**, 3510–3515.
15 C. Müller, J. Bergqvist, K. Vandewal, K. Tvingstedt, A. Anselmo, R. Magbnusson, M. Alonso, E. Moons, H. Arwin, M. Campoy-Quiles and O. Inganäs, *J. Mater. Chem.*, 2011, **21**, 10676–10684.
16 M. Koppe, H.-J. Egelhaaf, G. Dennler, M. C. Scharber, C. J. Brabec, P. Schilinsky and C. N. Hoth, *Adv. Funct. Mater.*, 2010, **20**, 338.
17 J. Peet, J. Y. Kim, N. E. Coates, W. L. Ma, D. Moses, A. J. Heeger and G. C. Bazan, *Nat. Mater.*, 2007, **6**, 497.
18 M. Morana, M. Wegscheider, A. Bonani, N. Kopidakis, S. Shaheen, M. Scharber, Z. Zhu, D. Waller, R. Gaudiana and C. Brabec, *Adv. Funct. Mater.*, 2008, **18**, 1757.

19 N. Li, F. Machui, D. Waller, M. Koppe and C. Brabec, *Sol. Energy Mater. Sol. Cells*, 2011, **95**, 3465–3471.
20 J. Zhao, A. Swinnen, G. van Assche and B. Van Mele, *J. Phys. Chem. B*, 2009, **113**, 1587–1591.
21 A. M. Ballantyne, T. A. M. Ferenczi, M. Campoy-Quiles, T. M. Clarke, A. Maurano, K. H. Wong, W. Zhang, N. Stingelin-Stutzmann, J.-S. Kim, D. D. C. Bradley, J. R. Durrant, I. McCulloch, M. Heeney and J. Nelson, *Macromolecules*, 2010, **43**, 1169–1174.
22 S. Malik and A. K. Nandi, *J. Polym. Sci., Part B: Polym. Phys.*, 2002, **40**, 2073–2085.
23 D. Kozub, K. Vakhshouri, L. Orme, C. Wang, A. Hexemer and E. Gomez, *Macromolecules*, 2011, **44**, 5722–5726.
24 B. Collins, E. Gann, L. Guignard, X. He, C. McNeill and H. Ade, *J. Phys. Chem. Lett.*, 2010, **1**, 3160–3166.
25 A. C. Mayer, M. F. Toney, S. R. Scully, J. Rivnay, C. J. Brabec, M. Scharber, M. Koppe, M. Heeney, I. McCulloch and M. D. McGehee, *Adv. Funct. Mater.*, 2009, **19**, 1173–1179.
26 P. P. Khlyabich, B. Burkhart and B. C. Thompson, *J. Am. Chem. Soc.*, 2011, **133**, 14534–14537.
27 S. Rathgeber, J. Perlich, F. Kühnlenz, S. Türk, H. Hoppe and R. Gehrke, *Polymer*, 2011, **52**, 3819–3826.
28 M. T. Dang, L. Hirsch and G. Wantz, *Adv. Mater.*, 2011, **23**, 3597–3602.
29 J. T. Roger, K. Schmidt, M. F. Toney, E. J. Kramer and G. C. Bazan, *Adv. Mater.*, 2011, **23**, 2284.
30 T. Erb, U. Zhokhavets, G. Gobsch, S. Raleva, B. Stühn, P. Schilinsky, C. Waldauf and C. J. Brabec, *Adv. Funct. Mater.*, 2005, **15**, 1193.
31 H. Azimi, A. Senes, M. Scharber, K. Hingerl and C. Brabec, *Adv. Energy Mater.*, 2011, **1**, 1162–1168.
32 F. Schauer, *Sol. Energy Mater. Sol. Cells*, 2005, **87**, 235–250.
33 V. Mihailetchi, J. Wildeman and P. Blom, *Phys. Rev. Lett.*, 2005, **94**, 126602.
34 N. Mott and R. Gurney, *Electronic Processes in Ionic Crystals*, Oxford University Press, London, 1940.
35 L. C. Palilis, M. Uchida and Z. H. Kafafi, *IEEE J. Sel. Top. Quantum Electron.*, 2004, **10**, 79–88, No. 1.
36 P. K. Watkins, A. B. Walker and G. L. B. Verschoor, *Nano Lett.*, 2005, **5**, 1814.
37 J. M. Frost, F. Cheynis, S. M. Tuladhar and J. Nelson, *Nano Lett.*, 2006, **6**, 1674.
38 I.-W. Hwang, S. Cho, J. Y. Kim, K. Lee, N. E. Coates, D. Moses and A. J. Heeger, *J. Appl. Phys.*, 2008, **104**, 033706.
39 F. C. Jamieson, T. Agostinelli, H. Azimi, J. Nelson and J. R. Durrant, *J. Phys. Chem. Lett.*, 2010, **1**, 3306.